

# **Design and optimization of a downhole coaxial heat exchanger for an enhanced geothermal system (EGS)**

**Yekoladio, P.J., Bello-Ochende\*, T. and Meyer J.P.**

Department of Mechanical and Aeronautical Engineering, University of Pretoria, Pretoria  
Private Bag X20, Hatfield 0028, South Africa.

## **Abstract**

The present study considers the design, performance analysis and optimization of a downhole coaxial heat exchanger for an enhanced geothermal system (EGS). The optimum mass flow rate of the geothermal fluid for minimum pumping power and maximum extracted heat energy was determined. In addition, the coaxial pipes of the downhole heat exchanger were sized based on the optimum geothermal mass flow rate and steady state operation. Transient effect or time-dependent cooling of the Earth underground, and the optimum amount and size of perforations at the inner pipe entrance region to regulate the flow of the geothermal fluid were disregarded to simplify the analysis. The paper consists of an analytical and numerical thermodynamic optimization of a downhole coaxial heat exchanger used to extract the maximum possible energy from the Earth's deep underground (2 km and deeper below the surface) for direct usage, and subject to a nearly linear increase in geothermal gradient with depth. The thermodynamic optimization process and entropy generation minimization (EGM) analysis were performed to minimize heat transfer and fluid friction irreversibilities. An optimum diameter ratio of the coaxial pipes for minimum pressure drop in both limits of the fully turbulent and laminar fully-developed flow regime was determined and observed to be nearly the same irrespective of the flow regime. Furthermore, an optimum geothermal mass flow rate and an optimum geometry of the downhole coaxial heat exchanger were determined for maximum net power output. Conducting an energetic and exergetic analysis to evaluate the performance of binary power cycle, higher Earth's temperature gradient and lower geofluid rejection temperatures were observed to yield maximum first- and second- law efficiencies.

\* Corresponding author. Tel.: +27 12 420 3105; Fax: +27 12 420 6632

---

E-mail: tunde.bello-ochende@up.ac.za

**Keywords:** Enhanced Geothermal System, Entropy Generation Minimization analysis, exergy analysis, downhole coaxial heat exchanger, binary cycle.

## **Nomenclature**

### **Alphabetic Symbols**

$A$	Heat transfer surface area, m <sup>2</sup>
$C$	Mass flow parameter
$C_p$	Specific heat capacity, J/kg.K
$D$	Diameter of pipes, m
$\dot{E}x$	Exergy flow, W
$f$	Fanning friction factor
$h$	Enthalpy, J/kg
$h$	Heat transfer coefficient, W/m <sup>2</sup> .K
$i$	Irreversibility, W
$K$	Local loss coefficient
$L$	Length of the downhole heat exchanger, m
$\dot{m}$	Mass flow rate, kg/s
$Nu$	Nusselt number
$P$	Pressure, Pa
$Pr$	Prandtl number
$\dot{Q}$	Heat transfer rate, W
$r$	Diameter ratio
$Re$	Reynolds number
$s$	Specific entropy, J/kg.K
$\dot{S}_{gen}$	Entropy generation rate, W/K
$\dot{S}'_{gen}$	Entropy generation rate per unit length, W/K.m
$St$	Stanton number
$Sv$	Svelteness
$T$	Fluid temperature, °C
$u$	Flow velocity, m/s
$\dot{W}$	Power generation, W
$x$	Axial distance along the tube/pipe, m

### **Greek symbols**

$\Delta$	Difference
$\chi$	Diameter ratio function
$\eta$	Efficiency, %
$\mu$	Dynamic viscosity, Pa.s
$\rho$	Fluid density, kg/m <sup>3</sup>
$\psi$	Specific exergy, J/kg
$\tau$	Dimensionless temperature difference

### **Subscripts**

<i>I</i>	First Law
<i>II</i>	Second Law
<i>0</i>	Reference state
<i>a</i>	Annular space
<i>D</i>	Diameter
<i>dest</i>	Destruction
<i>gen</i>	Generation
<i>geo</i>	Geothermal
<i>h</i>	Hydraulic
<i>i</i>	Inner
<i>in</i>	Inlet
<i>lam</i>	Laminar flow
<i>lm</i>	Logarithmic mean
<i>m</i>	Mean
<i>min</i>	Minimum
<i>net</i>	Net
<i>o</i>	Outer
<i>opt</i>	Optimum
<i>out</i>	Outlet
<i>rej</i>	Rejection
<i>rev</i>	Reversible
<i>turb</i>	Turbulent flow
<i>w</i>	Wall

## 1. Introduction

For decades, diverse studies have been conducted to develop renewable and sustainable energies while reducing the environment defects of global warming, greenhouse effect, air pollution and waste of natural resources. Among a diversity of energy-efficient and environmental friendly technologies identified for power generation, the geothermal energy has been proven itself to be an alternative energy source for electric power generation due to its economic competitiveness, operational reliability of its power plants, and its environmentally friendly nature [1].

The Earth's geothermal energy was originally conceived from the formation of planets, and is replenished at approximately 80% by radioactive decay of minerals (i.e. uranium, thorium and potassium) at a rate of 30 TW [2], and 20% by the residual heat from the Earth's interior such as volcanic activities and solar energy absorbed by the Earth surface [3,4]. Hence, the geothermal energy is the Earth's internal heat, naturally presents in the Earth's core, mantle and crust, and flows to the surface by conduction at a rate of 44.2 TW [5,6].

The International Energy Agency (IEA) [7] has estimated a worldwide geothermal installed capacity of 10,898 MW<sub>e</sub>, as of 2010, producing 67,246 MWh<sub>e</sub> per annum mostly from liquid-dominated geothermal reservoirs. This represents only 0.3% of the global electricity demand up to present. The electricity produced by means of geothermal energy is expected to increase significantly in the near future with the development of advanced geothermal energy extraction technologies able to extract more heat from the Earth's heat content rated at  $3 \times 10^{15}$  TWh [8,9].

Traditionally, the construction of geothermal power plants was restricted to areas near the edges of tectonic plates, volcanic sites, sedimentary hot sources as well as hot wet fractured granite. These regions contain subterranean hot water or steam reservoirs which facilitated hydrothermal energy flows either vertically by convection or horizontally through convection, advection and diffusion due to the difference in pressure of the extracted and re-injected geothermal fluid [5]. The active, high heat-flow areas comprise the region around the "Pacific Ring of Fire" (Central America, Indonesia, Japan, New Zealand, Philippines and the west cost of the United States), and the "Great Rift Valley" zones of Iceland, East of Africa and Eastern Mediterranean [10,11]. However, with the implementation of the binary cycles, the improvements in deep drilling and the development of more efficient heat extraction technologies, the exploitation of the heat energy was enabled by means of enhanced geothermal systems in all geological and geographical locations, irrespective of the presence of subterranean reservoirs of heated water or steam [5].

The hot-dry-rock geothermal energy consists of one or multiple injection and production wells, where the injected water is initially pressurized to cause hydraulic fracturing of hot, dry basement rocks. The technology has however, been proven to induce seismic activities and yet not economically viable, as the injected geothermal fluid is not harnessed in sufficient quantity for the production wells [5,12].

Advanced geothermal energy extraction technologies, implemented in Switzerland, Germany and Austria consist of a single gravel-filled well, closed-loop system where the heat transfer fluid is continuously circulated through the Earth in a closed pipe system without ever directly contacting the soil or water in which the loop is buried or immersed. The pipe dimensions, water circulation speed and the amount and size of perforations are optimized to ensure maximum extracted energy, which is dependent on the thermal conductivity of the rock or sediment [5].

Although various studies have been conducted in this regard, more focus was directed to resource exploration, reservoir stimulation, drilling techniques, and energy conversion systems. Energetic and exergetic analyses have been implemented to evaluate the performance of the geothermal energy based on the second law analysis. The studies aimed at reducing the cost of geothermal electricity production while investigating and optimizing the energy conversion systems of the geothermal power plants, to maximize the cycle power output [13,14]. Limited attention was paid to the second-law based performance criteria using entropy generation as the critical evaluation criteria for the design, performance analysis and optimization of the injection or/and production wells. Among others, Bejan [15] developed alternatives to thermodynamic performance and optimization of system subject to physical constraints such as entropy generation minimization (EGM), Yilmaz et al. [16] conducted a second-law based performance evaluation criteria using both entropy and exergy as evaluation parameters to assess the performance of heat exchangers. An elaborated investigation on energy extraction from fractured hot-dry-rock was conducted by Lim JS et al. [17] using the energy and exergy analysis. Their study determined under the effect of transient conduction, the optimum geothermal flow rate required to circulate water through the narrow fractures created in the subterranean hot-dry-rock bed to maximize the delivery of exergy over the lifetime of the hot-dry-rock system. A recent study conducted by Franco and Villani [18] has demonstrated, under given operating conditions, the strong dependency of the power cycle performance on the geothermal fluid temperature at the inlet and outlet of the resource wells, the energy conversion system being used, as well as the selection of the organic working fluid [19] employed in the conversion of low-grade geothermal

heat. Furthermore, DiPippo [20] concluded as follows: “The main design feature leading to a high-exergy efficiency lies in the design of the heat exchangers to minimize the loss of exergy during heat transfer processes. Another important feature that can result in high exergy efficiency is the availability of low-temperature cooling water that allows a once-through system for waste heat rejection.”

The purpose of this study is to design and optimize an energy extraction system for a downhole coaxial heat exchanger employed in an enhanced geothermal system, to maximize the cycle power output. The paper consists of an analytical and numerical thermodynamic optimization of a downhole coaxial heat exchanger used to extract maximum heat energy from the Earth’s deep underground (2 km and deeper below the surface) for direct usage, and subject to a nearly linear increase in geothermal gradient with depth. The Earth’s geothermal gradient, notably 2.4 to 4.8°C per 100 meter on average, is the natural increase of temperature with depth from the Earth’s surface and varies from different locations depending on the porosity and the degree of liquid saturation of the rock and sediments, their thermal conductivity and heat storage capacity, and the vicinity of magma chambers or heated underground reservoirs of liquid [5,21]. The study, however, focus on finding the optimum mass flow rate of the geothermal fluid for minimum pumping power, and maximum extracted heat energy; and was limited to the sizing of the coaxial pipes of the downhole heat exchanger for the optimum geofluid mass flow rate and steady state operation. Transient effect or time-dependent cooling of the Earth underground, and the optimum amount and size of perforations at the inner pipe entrance region to regulate the flow of the geothermal fluid were disregarded to simplify the analysis.

## **2. Model**

A binary cycle power plant with hot-dry-rock geothermal reservoir (Fig. 1a), operating with a moderately low-temperature and liquid-dominated geothermal resource in the range of 110°C to 160°C is considered. The primary heat transfer medium (e.g. water) is pumped at high pressure and continuously circulated through the Earth in a closed pipe system [22,23]. The fluid is heated by the linearly increasing underground temperature with depth, as it flows down the well. A secondary or binary fluid with a lower boiling point and higher vapour pressure is thereafter completely vaporized or usually superheated by the primary fluid through a closed pipe system heat exchanger, then expanded in the turbine and condensed either in an air-cooled or water-cooled condenser prior returning to the vaporizer and thus completing the Rankine cycle [24].

The downhole coaxial heat exchanger for an enhanced geothermal system consists of a single gravel-filled well, closed-loop system where the heat transfer fluid is continuously circulated through the Earth in a closed pipe system without ever directly contacting the soil or water in which the loop is buried or immersed (Fig. 1b). The cold water is thus pumped downward through the annular space, and heated across the annular wall by the increasingly warmer rock material, as it flows downward. The heated stream returns, eventually to the surface through the inner pipe, which is effectively insulated to minimize any potential loss of heat to the surrounding.

### **3. Analytical method**

#### **3.1. Assumptions**

The following assumptions were made:

1. The underground temperature increases almost linearly with depth from the Earth's surface. Hence, a constant wall heat flux is assumed on the outer diameter of the downhole coaxial heat exchanger;
2. The outer pipe of the downhole coaxial heat exchanger has a thin wall and is highly conductive. Consequently, its thermal resistance is negligible;
3. An effective layer of insulation onto the wall of the inner pipe ensures negligible heat transfer from the upflowing hot stream through the inner pipe to the downflowing cold stream in the annular space of the downhole coaxial heat exchanger;
4. The geothermal fluid collected from the downhole heat exchanger, is at a saturation liquid state;
5. All control volumes operate under steady-state condition.

#### **3.2. Constraints, design variables and operating parameters**

The thermodynamic performance of the downhole coaxial heat exchanger was assessed for a nearly linear increase with depth of the underground temperature gradient  $dT / dx$  to simplify the analysis. Consequently, a constant wall heat flux was assumed on the outer diameter of the downhole coaxial heat exchanger. In addition, the local pressure loss at the lower extremity of the well was verified to be negligible for a coaxial pipes length greater than twenty times its diameter.

Although various design variables need to be considered while designing for a downhole coaxial heat exchanger, this study has considered a few in the thermodynamic optimization process,

namely the diameter ratio of the coaxial pipes, the geofluid circulation mass flow rate, and the outer diameter of the downhole coaxial heat exchanger.

Table 1 gives the operating parameters, typically the dead or reference state, inlet and outlet temperatures range of the geothermal fluid, and the Earth's underground temperature gradient on the outer diameter of the downhole coaxial heat exchanger.

Parameters	$P_o$ [kPa]	$T_o$ [ $^{\circ}C$ ]	$T_{rej}$ [ $^{\circ}C$ ]	$T_{geo}$ [ $^{\circ}C$ ]	$(dT/dx)$ [ $^{\circ}C/100m$ ]
	100	25	50 -110	110 - 160	2.4 – 4.8

Table 1: Operating parameters used in the simulation

### 3.3. Pressure loss analysis

The optimization process began with an investigation of a potential local pressure loss [25], at the lower extremity of the well, caused by the sudden change in flow direction of the heated stream from the annular space of the downhole coaxial heat exchanger into the inner pipe to return to the surface. This effect led to recirculation of the geofluid immediately downstream to the inner pipe entrance.

The local pressure drop is given by [26]

$$\Delta P_{local} = \frac{1}{2} K \rho U_i^2 \quad (1)$$

where the local loss coefficient was approximated as a sudden contraction,

$$K = 0.45 \left[ 1 - \left( \frac{D_i}{D_o} \right)^2 \right] \quad (2)$$

Defining the distributed losses as due to fully developed flow in the inner pipe, as

$$\Delta P_{distributed} = f_i \frac{4L_i}{D_i} \left( \frac{1}{2} \rho U_i^2 \right) \quad (3)$$

The ratio of pressure drops is expressed by

$$\frac{\Delta P_{local}}{\Delta P_{distributed}} = \frac{0.45 \left[ 1 - \left( \frac{D_i}{D_o} \right)^2 \right]}{f_i \frac{4L_i}{D_i}} \quad (4)$$

The svelteness of the flow geometry is defined by Bejan [25] as follow

$$Sv = \frac{\text{external flow length scale}}{\text{internal flow length scale}} \cong \left( \frac{4}{\pi} \right)^{\frac{1}{3}} \left( \frac{L_i}{D_i} \right)^{\frac{2}{3}} \quad (5)$$

Thus, in term of svelteness, Eq. (4) is rewritten as

$$\frac{\Delta P_{local}}{\Delta P_{distributed}} = \frac{0.45 \left[ 1 - \left( \frac{D_i}{D_o} \right)^2 \right]}{4 f_i \left( \frac{4}{\pi} \right)^{\frac{1}{2}} S_v^{\frac{3}{2}}} \quad (6)$$

If the flow in the inner pipe is in the laminar fully-developed flow regime, then the fanning friction factor is a function of the Reynolds number and given by [27]

$$f_i = \frac{16}{\text{Re}_i} \quad (7)$$

Substituting Eq. (7) into Eq. (6) and assuming that the ratio of the inner to the outer diameter of the coaxial pipes is much less than 1, the following equation was obtained

$$\left( \frac{\Delta P_{local}}{\Delta P_{distributed}} \right)_{lam} \cong \frac{\left( \frac{\text{Re}_i}{126} \right)}{S_v^{\frac{3}{2}}} \quad (8)$$

From Eq. (8), the ratio of pressure drops is seen to be directly proportional to the inner pipe flow Reynolds number and inversely proportional to the svelteness. Hence, for  $S_v \gg 0.04 \text{Re}_i^{\frac{2}{3}}$ , the local pressure loss at the lower extremity of the well could be neglected in the laminar fully-developed flow regime.

Similarly, if the flow is in the fully turbulent and fully rough regime, the friction factor is thus a constant and independent of the Reynolds number. Using the explicit approximation for smooth ducts [26]

$$f \cong 0.046 \text{Re}^{-\frac{1}{5}} \quad (10^4 < \text{Re} < 10^6) \quad (9)$$

Assuming that the fanning friction factor is of order 0.01 [26], the ratio of pressure drops in the fully turbulent and fully rough regime is expressed as,

$$\left( \frac{\Delta P_{local}}{\Delta P_{distributed}} \right)_{turb} \cong \frac{12.7}{S_v^{\frac{3}{2}}} \quad (10)$$

Consequently, for  $S_v \gg 5.44$ , the local pressure loss at the lower extremity of the well could be neglected in the fully turbulent and fully rough regime.

The variation of the ratio of the pressure drops to the svelteness, for both laminar and turbulent fully-developed flow regimes was plotted in Fig. 2. As the svelteness increases, the ratio of the

pressure drops decreases drastically. At the upper limit of the turbulent fully-developed flow regime and for Svelteness much greater than eight, the ratio of the pressure drops is minimum. Hence, from Eq. (5), it could be proved that the local pressure loss at the lower extremity of the well could be neglected, irrespective of the flow regime, for a coaxial pipe length greater than twenty times its diameter.

### 3.4. Optimum diameter ratio

For an inner diameter of the coaxial pipes much smaller than its outer diameter, it could be observed that the stream will be “strangled” as it flows upward through the inner pipe. On the contrary, that is the inner diameter being nearly as large as the pipe outer diameter, the flow will be hindered by the narrowness of the annular space [22, 28]. In both cases, the total pressure drop to be overcome by the pump is extremely excessive. Hence, the need of determining an optimum diameter ratio of the coaxial pipes is essential to ensure minimum total pressure drop, thus minimum pumping power requirement.

The pressure drop per unit length in the inner pipe flow section of the downhole coaxial heat exchanger is given by [26]

$$\left(\frac{\Delta P}{L}\right)_i = \frac{2\rho}{D_o^5} \left(\frac{4}{\pi}\right)^2 \left(\frac{\dot{m}}{\rho}\right)^2 \frac{f_i}{r^5} \quad (11)$$

where the diameter ratio  $r$  is defined as

$$r = \frac{D_i}{D_o} \quad (12)$$

Similarly, the pressure drop per unit length in the annular space region of the downhole coaxial heat exchanger can be expressed by

$$\left(\frac{\Delta P}{L}\right)_a = \frac{2\rho}{D_o^5} \left(\frac{4}{\pi}\right)^2 \left(\frac{\dot{m}}{\rho}\right)^2 \frac{f_a}{(1-r)^3(1+r)^2} \quad (13)$$

Thus, the total pressure drop per unit length contributed by each portion of the coaxial pipe is

$$\left(\frac{\Delta P}{L}\right)_{total} = \left(\frac{\Delta P}{L}\right)_a + \left(\frac{\Delta P}{L}\right)_i = \frac{1}{\rho} \left(\frac{\dot{m}}{\pi}\right)^2 \left(\frac{2}{D_o}\right)^5 \mathcal{X}_{urb} \quad (14)$$

where,

$$\mathcal{X}_{urb} = \frac{f_a}{(1-r)^3(1+r)^2} + \frac{f_i}{r^5} \quad (15)$$

Eq. (15) can be minimized with respect to the diameter ratio  $r$ , to obtain the minimum total pressure drop and pumping power requirement.

In the large Reynolds number limit of the fully turbulent and fully rough regime, where the friction factors of both the inner pipe and annular space are constant and independent of the Reynolds number, an optimum diameter ratio of the coaxial pipes was obtained numerically as

$$r_{opt,turb} = 0.653 \quad (16)$$

In the laminar fully-developed flow regime, however, the friction factors being strongly dependent on the Reynolds number, are defined by [27]

$$f_i = \frac{16}{\text{Re}_i} = \frac{16\mu\left(\frac{\pi}{4}\right)rD_o}{\dot{m}} \quad (17)$$

$$f_a = \frac{16\mu\left(\frac{\pi}{4}\right)(1-r)D_o}{\dot{m}} \frac{(1-r)^2(1-r^2)}{1-r^4 - \frac{(1-r^2)^2}{\ln\left(\frac{1}{r}\right)}} \quad (18)$$

Substituting Eqs. (17)-(18) into Eq. (12) , the following equation of the total pressure drop per unit length contributed by each portion of the coaxial pipes in the laminar fully-developed flow regime was obtained

$$\left(\frac{\Delta P}{L}\right)_{total,lam} = \frac{\mu}{\rho} \left(\frac{\dot{m}}{\pi}\right) \left(\frac{2^7}{D_o^4}\right) \mathcal{X}_{lam} \quad (19)$$

where,

$$\mathcal{X}_{lam} = \frac{\frac{1-r}{1+r}}{1-r^4 - \frac{(1-r^2)^2}{\ln\left(\frac{1}{r}\right)}} + \frac{1}{r^4} \quad (20)$$

Minimizing Eq. (20) with respect to the diameter ratio, one could obtain numerically

$$r_{opt,lam} = 0.683 \quad (21)$$

The same result can eventually be obtained numerically by assuming that the annular space is identical to a parallel-plate geometry positioned  $\frac{(D_o - D_i)}{2}$  apart. Hence, the annular friction factor is given by [22]

$$f_a = \frac{16}{\text{Re}_a} = \frac{16\mu\left(\frac{\pi}{4}\right)D_o(1-r)}{\dot{m}} \quad (22)$$

And the total pressure drop as

$$\left(\frac{\Delta P}{L}\right)_{total,lam} = \frac{\mu}{\rho}\left(\frac{\dot{m}}{\pi}\right)\left(\frac{2^5}{D_o^4}\right)\mathcal{X}_{lam} \quad (23)$$

where,

$$\mathcal{X}_{lam} = \frac{24}{(1-r)^2(1+r)^2} + \frac{16}{r^4} \quad (24)$$

Eq. (24) can be minimized with respect to the diameter ratio to give the same result as in Eq. (21).

In brief, from Eqs. (16) and (21), the optimum diameter ratio of the coaxial pipes to yield minimum total pressure drop and minimum pumping power requirement, is observed to be nearly the same in both limits of the fully turbulent and laminar fully-developed flow regimes. That is, for a given outer diameter of the downhole coaxial heat exchanger, a corresponding inner diameter will be the same irrespective of the flow regime.

### 3.5. Entropy Generation Minimization (EGM) analysis

The entropy generation, as defined by Bejan [25], represents the measure of imperfection. Hence, minimizing the entropy generation term will yield maximum extracted heat energy for a given underground temperature gradient, according to Gouy-Stodola relation [30].

The mass balance (or continuity) equation is given by [29]

$$\sum \dot{m}_{in} = \sum \dot{m}_{out} = \dot{m} \quad (25)$$

Thus, the rate of entropy generation is related to the rate of entropy transfer as

$$\dot{S}_{gen} = \dot{m}(s_{out} - s_{in}) - \frac{\dot{Q}}{T_w} \quad (26)$$

Using thermodynamic relations [29,31] outlined below, and the incompressibility property of the geofluid (i.e. water)

$$dh = CpdT \quad (27)$$

$$Tds = dh - \frac{dP}{\rho} \quad (28)$$

$$d\dot{Q} = \dot{m}dh \quad (29)$$

The entropy generation rate per unit length of the downhole coaxial heat exchanger is given by

$$\dot{S}'_{gen} = \dot{m}Cp \frac{\Delta T}{T_m^2(1+\tau)} \left( \frac{dT}{dx} \right) + \frac{\dot{m}}{\rho T_m} \left( -\frac{dP}{dx} \right) \quad (30)$$

Eq. (30) can be rewritten as [16]

$$\dot{S}'_{gen} = \dot{S}'_{gen,\Delta T} + \dot{S}'_{gen,\Delta P} \quad (31)$$

The first term represents the entropy generation rate per unit length due to heat transfer irreversibility across a finite temperature difference along the outer wall of the annular space, while the inner pipe is effectively insulated to minimize any potential loss of heat to the surrounding. And the second term accounts for the total fluid friction irreversibility as a result of the downward flow of the geofluid through the annular space then upward through the inner pipe, to return to the surface.

In Eq. (30),  $\Delta T$  represents the temperature difference between the outer wall of the annular space and the mean temperature of the stream, i.e.  $\Delta T = T_w - T_m$ . Under the assumptions of uniform wall heat flux, constant fluid properties and fully developed flow regimes, both the outer wall and mean fluid temperatures increase linearly in the flow direction. Consequently, the local temperature difference between the wall and the stream does not change along the flow direction.

Considering an energy balance of a control volume of length  $dx$  of the coaxial pipes, the total rate of convective heat transfer is given by [22]

$$\dot{Q} = \dot{m}.Cp.dT = h.\pi D_o dx.\Delta T_{lm} \quad (32)$$

Hence the temperature difference  $\Delta T$ , between the outer wall of the annular space and the mean temperature of the stream, increases linearly with the mean temperature gradient, and inversely with the convective heat transfer coefficient  $h$ , according to

$$\Delta T = \Delta T_{lm} = \frac{\dot{m}Cp}{h\pi D_o} \left( \frac{dT}{dx} \right) \quad (33)$$

Assumption that  $\tau = \frac{\Delta T}{T_m} \ll 1$ , the substitution of Eq. (33) into Eq. (30) yields

$$\dot{S}'_{gen} = \frac{\dot{m}^2 Cp^2}{h\pi D_o T_m^2} \left( \frac{dT}{dx} \right)^2 + \frac{\dot{m}}{\rho T_m} \left( -\frac{dP}{dx} \right) \quad (34)$$

Since heat transfer occurs only across the outer wall of the annular space, the following equations from heat transfer principles apply [22]

$$h_a = St.\rho.Cp.u_a \quad (35)$$

$$Nu_a = \frac{hD_h}{k} = St \cdot Re_a \cdot Pr \quad (36)$$

$$u_a = \frac{4\dot{m}}{\rho\pi D_h^2} \quad (37)$$

Where

$$D_h = D_o - D_i = D_o(1-r) \quad (38)$$

Substituting Eqs. (35)-(38) into Eq. (30) and integrating along the length of the heat exchanger for a constant increment of the underground temperature with depth, the entropy generation rate per unit length can be expressed by

$$\dot{S}'_{gen} = \frac{\dot{m}Cp Re_a Pr D_o (1-r)^2}{4Nu_a T_m^2} \left(\frac{dT}{dx}\right)^2 + \frac{\dot{m}}{\rho T_m} \left(-\frac{\Delta P}{L}\right)_{total} \quad (39)$$

In the large Reynolds number limit of the fully turbulent and fully rough regime, the Nusselt number of the flowing geothermal fluid in the annular space of the coaxial pipes was approximated by Petukhov and Roizen correlation [32] for heat transfer at the outer wall of a concentric annular duct with its inner wall well-insulated, as

$$\frac{Nu_a}{Nu_i} = 1 - 0.14 \left(\frac{D_i}{D_o}\right)^{0.6} \quad (40)$$

Where the Nusselt number of the upflowing stream in the inner pipe is given by [22]

$$Nu_i \cong 0.023 Re_i^{0.8} Pr^{0.4} \quad (0.7 < Pr < 160, Re_i > 10^4) \quad (41)$$

Substituting Eqs. (9), (14)-(15) and (40)-(41) into Eq. (39), the following equation was obtained

$$\dot{S}'_{gen,turb} = \frac{10.87\dot{m}Cp Re_a Pr^{0.6} D_o (1-r)^2}{(1-0.14r^{0.6}) T_m^2 Re_i^{0.8}} \left(\frac{dT}{dx}\right)^2 + \frac{1.472\dot{m}^3}{\pi^2 \rho^2 T_m D_o^5} \left( \frac{Re_a^{\frac{1}{5}}}{(1-r)^3(1+r)} + \frac{Re_i^{\frac{1}{5}}}{r^5} \right) \quad (42)$$

The dimensionless Reynolds numbers for flow through straight pipes in terms of the pipe outer diameter are given by

$$Re_a = \frac{4\dot{m}}{\pi\mu D_o(1-r)} \quad (43)$$

$$Re_i = \frac{4\dot{m}}{\pi\mu r D_o} \quad (44)$$

Expressing Eq. (42) in terms of the Reynolds number of the flow in the annular space by substituting Eqs. (43)-(44) and eliminating  $D_o$ , the following equation was obtained

$$\dot{S}'_{gen,turb} = \frac{13.84\dot{m}^2 Cp Pr^{0.6} (1-r)^{0.2} \left(\frac{dT}{dx}\right)^2}{\mu \left(\frac{1}{r^{0.8}} - \frac{0.14}{r^{0.2}}\right) T_m^2 Re_a^{0.8}} + \frac{0.0446 Re_a^{4.8} \mu^5 (1-r)^{4.8}}{\rho^2 T_m \dot{m}^2} \left( \frac{1}{(1-r)^{2.8} (1+r)^2} + \frac{1}{r^{4.8}} \right) \quad (45)$$

Eq. (45) was differentiated with respect to the geofluid mass flow rate and equalled to zero. The optimum mass flow rate of the geothermal fluid under turbulent flow conditions was determined for minimum entropy generation, thus maximum extracted heat energy for a given underground temperature gradient. The following relations were obtained

$$\dot{m}_{opt,turb} = 0.238 Re_a^{1.4} C_{turb}^{0.25} \quad (46)$$

where,

$$C_{turb} = \frac{\mu^6 T_m}{\rho^2 Cp Pr^{0.6} \left(\frac{dT}{dx}\right)^2} (1-r)^{4.6} \left(\frac{1}{r^{0.8}} - \frac{0.14}{r^{0.2}}\right) \left( \frac{1}{(1-r)^{2.8} (1+r)^2} + \frac{1}{r^{4.8}} \right) \quad (47)$$

In the laminar fully-developed flow regime, the Nusselt number of the flowing geothermal fluid in the annular space of the coaxial pipes was approximated by Martin's correlation [32] for heat transfer at the outer wall of a concentric annular duct with inner wall well-insulated, as

$$Nu_a = 3.66 + 1.2 \left(\frac{D_i}{D_o}\right)^{0.5} \quad \left( 0.1 < Pr < 10^3, Re_D < 2300, 0 < \frac{D_i}{D_o} < 1 \right) \quad (48)$$

Substituting Eqs. (17)-(20) and (48) into Eq. (39), the following equation was obtained

$$\dot{S}'_{gen,lam} = \frac{\dot{m} Cp Re_a Pr D_o (1-r)^2 \left(\frac{dT}{dx}\right)^2}{4(3.66 + 1.2r^{0.5}) T_m^2} + \frac{128\dot{m}^2 \mu}{\pi \rho^2 T_m D_o^4} \left( \frac{\frac{1-r}{1+r}}{1-r^4 - \frac{(1-r^2)^2}{\ln\left(\frac{1}{r}\right)}} + \frac{1}{r^4} \right) \quad (49)$$

Expressing Eq. (49) in terms of the Reynolds number of the flow in the annular space and eliminating  $D_o$ , the following equation was obtained

$$\dot{S}'_{gen,lam} = \frac{0.318\dot{m}^2 Cp Pr (1-r) \left(\frac{dT}{dx}\right)^2}{\mu (3.66 + 1.2r^{0.5}) T_m^2} + \frac{15.50 Re_a^4 \mu^5 (1-r)^4}{\rho^2 T_m \dot{m}^2} \left( \frac{\frac{1-r}{1+r}}{1-r^4 - \frac{(1+r^2)^2}{\ln\left(\frac{1}{r}\right)}} + \frac{1}{r^4} \right) \quad (50)$$

Similarly, Eq. (50) was differentiated with respect to the geofluid mass flow rate and equalled to zero. The optimum mass flow rate of the geothermal fluid was determined under laminar flow conditions, as

$$\dot{m}_{opt,lam} = 2.642 \text{Re}_a C_{lam}^{0.25} \quad (51)$$

where,

$$C_{lam} = \frac{\mu^6 T_m}{\rho^2 C_p \text{Pr} \left( \frac{dT}{dx} \right)^2} (1-r)^3 (3.66 + 1.2r^{0.5}) \left( \frac{\frac{1-r}{1+r}}{1-r^4 - \frac{(1+r^2)^2}{\ln\left(\frac{1}{r}\right)}} + \frac{1}{r^4} \right) \quad (52)$$

Varying the Reynolds number of the flow in the annular space from the laminar to the turbulent limits, an optimum mass flow rate of the geothermal fluid was obtained from Eqs. (46) and (51). The outer diameter of the downhole coaxial heat exchanger was thereafter determined from Eq. (43) as

$$D_o = \frac{4\dot{m}_{opt}}{\pi\mu(1-r)\text{Re}_a} \quad (53)$$

### 3.6. Performance analysis of a binary power cycle: Energy and Exergy analyses

Performing an energy and exergy analyses to assess the performance of a geothermal binary power cycle, based on the inlet heat resource and rejection conditions of the geothermal fluid leaving and entering the downhole coaxial heat exchanger respectively, the first- and second-law efficiencies with respect to the reference temperature  $T_o$ , are given by [20,24,33]

$$\eta_I = \frac{\text{net work output}}{\text{total energy inputs}} = \frac{\dot{W}_{net}}{\dot{m}_{geo}(h_{geo} - h_o)} \quad (54)$$

$$\eta_{II} = \frac{\text{net work output}}{\text{total exergy inputs}} = \frac{\dot{W}_{net}}{\dot{m}_{geo}[(h_{geo} - h_o) - T_o(s_{geo} - s_o)]} \quad (55)$$

where

$$\dot{W}_{net} = \dot{W}_{rev} - \dot{I} \quad (56)$$

$$\dot{W}_{rev} = \dot{E}x_{in} = \dot{m}_{geo} Cp \left[ (T_{geo} - T_{rej}) - T_o \ln \left( \frac{T_{geo}}{T_{rej}} \right) \right] \quad (57)$$

$$\dot{I} = \dot{E}x_{dest} = T_o \dot{S}_{gen} \quad (58)$$

Eqs. (54) and (55) represent the maximum limit of the energetic and exergetic availability of a geothermal resource, respectively, based on the geothermal fluid state at the inlet of the primary heat exchanger, and corresponding to the theoretical lower limit temperature of the rejection geofluid, known as the reference state.

#### 4. Model validation

The numerical results obtained, were validated with the work of Franco and Villani [18] who did perform an energy and exergy analyses to determine the upper limit to the first and second- law efficiency, based on the geothermal fluid state at the inlet of the primary heat exchanger. The results in Fig. 3 illustrate a very good agreement. It is worth mentioning that the latter work [18] assumed zero lost work, thus zero entropy generation rate; whereas the present work used the minimum entropy generation rate produced by the system, which is, however, approaching zero as discussed in section 5.

#### 5. Results and discussion

As pointed out by Lim JS et al. [17], there exists an optimum geothermal mass flow rate at which heat energy is extracted from a given hot-dry-rock system to produce maximum net power output. In the extreme cases of faster and slower circulation of the geothermal fluid, the resultant exergy is much lower due to no temperature raise of the rapidly flowing geothermal fluid or the lower mass flow rate, respectively. Hence, the objective of this paper was to determine the optimum geothermal mass flow rate for an enhanced geothermal system to generate both minimum pressure drop and entropy generation, while maximizing the extracted heat energy.

The variation of the optimum mass flow rate of the geothermal fluid in the laminar fully-developed flow regime, and the large Reynolds number limit of the fully turbulent and fully rough regime is shown in Fig. 4 for a given inlet heat resource and geothermal rejection temperature of 160°C and 50°C, respectively. In Fig. 5, the geothermal rejection temperature was fixed at 50°C and the inlet heat resource temperature varied for a given mean underground temperature gradient of 3.5°C per 100m. Both figures illustrate an increase in optimum mass flow rate with the increase in the Reynolds number. The increment in the optimum mass flow

rate is, however, exponential at low Reynolds number compared to nearly linear at very large Reynolds number. A possible reason of such behaviour is the dependency of the fluid friction factor on the Reynolds number in the laminar region, whereas it is constant and independent on the Reynolds number in the fully turbulent and fully rough regime. Furthermore, the optimum mass flow rate of the geothermal fluid was observed to decrease with the increase in either the underground temperature gradient (Fig. 4) or the inlet heat resource temperature (Fig. 5). In other words, maximum power output can be achieved from higher underground temperature gradients or higher temperature geothermal resources.

In Figs. 6 and 7, the variation of the coaxial pipes outer diameter was plotted against the Reynolds number for a variation in underground temperature gradient and inlet geothermal resource temperature, respectively. A substantial variation of the geometry size was observed with the Earth's underground temperature gradient, rather with the geothermal resource temperature. Hence, geological and geographical regions with high Earth's underground temperature gradients will result in a substantial decrease in the size of the downhole coaxial heat exchanger to achieve a given cycle power output, thus lowering the cost of the power plant.

In Fig. 8, the minimum entropy generation rate per unit length of the downhole coaxial heat exchanger was plotted against the Reynolds number for a given inlet heat resource and geothermal rejection temperature of 160°C and 50°C, respectively. The minimum entropy generation rate was observed to increase exponentially with the Reynolds number in both regions of the laminar and turbulent fully-developed flow regimes, to yield values approaching zero even at large Reynolds numbers limit of the fully turbulent and fully rough regime.

The first- and second-law efficiencies with respect to the reference temperature  $T_o$ , were plotted in Figs. 9 and 10, respectively, as a function of the geothermal rejection temperature and at a given mean underground temperature gradient of 3.5°C per 100m. The first-law efficiency, representing a quantitative measure of the effectiveness of the conversion of the available geothermal energy into useful work, as discussed by Subbiah and Natarajan [34], is observed to be as little as 20% maximum (Fig. 9). This is justified by the moderately low temperature of the liquid-dominated geothermal resource considered to be in the range of 110°C to 160°C. The second-law efficiency on the other hand, could be rated to more than 50% (Fig. 10) since it accounts for the overall exergy inputs to the cycle with reference to the dead state environmental design conditions [34]. In addition, it was observed that both the first- and second- law efficiencies decreased with the increase in the geothermal rejection temperature, as it was varied

from the lower limit temperature of the reference state to the upper limit temperature of the inlet geothermal resource. The first- and second- law efficiencies were also maximum for higher inlet geothermal resource temperature. Hence, maximum first- and second- law efficiencies can be obtained with a combination of high inlet geothermal resource temperatures and low geofluid rejection temperatures. While the former is dependent on the site underground temperature gradient and the depth of the coaxial downhole heat exchanger to reach higher underground base temperatures, the latter is, however, limited by the dead state environmental design conditions.

## **6. Conclusions**

A thermodynamic design and optimization of a downhole coaxial heat exchanger for an enhanced geothermal system was considered. The optimum diameter ratio of the coaxial pipes was determined for minimum pressure drop in both limits of the fully turbulent and laminar fully-developed flow regimes. It was observed to be nearly the same irrespective of the flow regime. Performing an entropy generation minimization analysis, the entropy generation rate was found to be due to both heat transfer and fluid friction irreversibilities. The coaxial pipes dimensions and geofluid circulation flow rate were optimized to ensure minimum pumping power requirement and maximum extracted heat energy from the Earth's deep underground. It was deduced that a higher underground temperature gradient minimize both the geometry size of the downhole heat exchanger and the geothermal mass flow rate required to be continuously circulated through the Earth. Although most of the studies conducted in this topic have ignored the size of the borehole due to its slenderness as compared to the vast Earth geometry and due the computation difficulties associated with the design of a downhole coaxial heat exchanger as demonstrated throughout this paper, an optimum design of the coaxial pipes can substantially lower the drilling and exploitation costs of the geothermal power plant. Finally, the energetic and exergetic analyses were conducted to assess the performance of a geothermal binary power cycle. In brief, the first- and second- law efficiencies were maximized for a combination of high inlet geothermal resource temperatures and low geofluid rejection temperatures.

## **Acknowledgements**

The funding obtained from NRF, University of Pretoria and Hitachi Power Africa is acknowledged and duly appreciated.

## **References**

- [1] DiPippo, R 1998, 'Geothermal Power Systems', in Elliott, TC, Chen, K & Swanekamp, RC, *Standard handbook of power plant engineering*, 2<sup>nd</sup> edn, MacGraw-Hill, New York, pp. 8.27 - 8.60.
- [2] Rybach, L 2007, 'Geothermal Sustainability', <http://geoheat.oit.edu/bulletin/bull28-3/art.pdf>, *Geo-Heat Centre Quarterly Bulletin* (Klamath Falls, Oregon: Oregon Institute of Technology), vol. 28, no. 3, pp. 2-7, ISSN 0276-1084 (<http://www.worldcat.org/issn/0276-1084>), <http://geoheat.oit.edu/bulletin/bull28-3/art.pdf>, retrieved 2009-05-09.
- [3] Alfe, D, Gillan, MJ & Price, GD 2003, 'Thermodynamics from first principles: temperature and composition of the Earth's core', *Mineralogical Magazine*, vol. 67, no. 1, pp. 113–123.
- [4] Turcotte, DL & Schubert, G 2002, *Geodynamics*, 2nd edn, Cambridge, England, UK: Cambridge University Press. pp. 136–137.
- [5] Bassfeld Technology Transfer 2009, *Geothermal Power Generation: Economically viable electricity generation through advanced geothermal energy technologies*, Switzerland.
- [6] Pollack, HN, Hurter, SJ & Johnson, JR 1993, 'Heat flow from the Earth's interior: Analysis of the Global Data Set', <http://www.agu.org/pubs/crossref/1993/93RG01249.shtml>, Rev, *Geophys*, vol. 30, no. 3, pp. 267-280, <http://www.agu.org/pubs/crossref/1993/93RG01249.shtml>.
- [7] EIA 2010, *International Energy Outlook 2010*, Report No.: DOE/EIA-0484(2010). U.S. Energy Information Administration, Washington, 338 pp.
- [8] Fridleifsson, IB, Bertani, R, Huenges, E, Lund, JW, Ragnarsson, A, Rybach, L, Homhmeyer, O & Trittin, T 2009, *The possible role and contribution of geothermal energy to the mitigation of climate change*, ([http://iga.igg.cnr.it/documenti/IGA/Fridleifsson\\_et\\_al\\_IPCC\\_Geothermal\\_paper\\_2008.pdf](http://iga.igg.cnr.it/documenti/IGA/Fridleifsson_et_al_IPCC_Geothermal_paper_2008.pdf)), Luebeck, Germany, pp.59-80. [http://iga.igg.cnr.it/documenti/IGA/Fridleifsson\\_et\\_al\\_IPCC\\_Geothermal\\_paper\\_2008.pdf](http://iga.igg.cnr.it/documenti/IGA/Fridleifsson_et_al_IPCC_Geothermal_paper_2008.pdf), retrieved 2009-04-06.
- [9] Bertani, R 2012, 'Geothermal power generation in the world 2005-2010 update report', *Geothermics*, vol. 41, no.1, pp. 1-29.
- [10] IEA ETSAP 2010, *Geothermal heat and power*, May 2010 edition, Energy Technology Systems Analysis Programme, USA.
- [11] Geothermal Energy Association 2010, *Geothermal Energy: International Market Update*, Geothermal Energy Association, Washington.
- [12] Tester, JW et al. 2006, *The Future of Geothermal Energy, Impact of enhanced geothermal systems (EGS) on the United States in the 21st Century: An Assessment*, Idaho National Laboratory, Idaho Falls, pp. 1–8 to 1–33.

- [13] EERE 2009, *Geothermal Technologies Program – Recovery Act Funding Opportunities*, Energy Efficiency & Renewable Energy, USA, 59 pp.
- [14] Kutscher, FC 2000, *The Status and future of geothermal electric power*, American Solar Energy Society Conference, Madison, June 16-21, 2000, National Renewable Energy Laboratory, Colorado.
- [15] Bejan, A 1999, 'Thermodynamic optimization Alternatives: Minimization of Physical Size Subject to Fixed Power', *International Journal of Energy Research*, vol. 23, no. 1, pp. 1111-1121.
- [16] Yilmaz, M, Sara, ON & Karsli, S 2001, 'Performance evaluation criteria for heat exchangers based on the second law analysis', *Exergy, an International Journal*, vol. 4, no. 1, pp. 278-294.
- [17] Lim, JS, Bejan, A & Kim, JH 1992, 'Thermodynamics of energy extraction from fractured hot dry rock', *International journal of heat and fluid flow*, vol. 13, no. 1, pp. 71-77.
- [18] Franco, A & Villani, M 2009, 'Optimum design of binary cycle power plants for water-dominated, medium-temperature geothermal fields', *Geothermics*, vol. 38, no.1, pp. 379-391.
- [19] Madhawa, HD, Mihajlo, G, Worek, WM & Yasuyuki, I 2007, 'Optimum design criteria for an organic Rankine cycle using low temperature geothermal heat sources', *Energy*, vol. 32, no. 1, pp. 1698–706.
- [20] DiPippo, R 2004, 'Second Law assessment of binary plants generating power from low-temperature geothermal fluids', *Geothermics*, vol. 33, no.1, pp. 565–86.
- [21] Fridleifsson, Ingvar B., Bertani R., Huenges E., Lund, JW., Ragnarsson A., Rybach L., Hohmeyer O. & Trittin T. 2009, The possible role and contribution of geothermal energy to the mitigation of climate change, Luebeck, Germany, pp. 59–80.
- [22] Bejan, A 1993, *Heat transfer*, Wiley, New York.
- [23] Yari, M 2010, 'Exergetic analysis of various types of geothermal power plants', *Renewable Energy*, vol. 35, no. 1, pp. 112-121.
- [24] Kanoglu, M & Bolatturk, A 2008, 'Performance and parametric investigation of a binary geothermal power plant by exergy', *Renewable Energy*, vol. 33, no. 1, pp. 2366–74.
- [25] Bejan, A & Lorente, S 2008, *Design with constructal theory*, John Wiley & Sons, New Jersey.
- [26] Bejan, A, Tsatsaronis, G & Moran, M 1996, *Thermal design and optimization*, Wiley, New York.
- [27] White, FM 2008, *Fluid mechanics*, 6<sup>th</sup> edn, McGraw-Hill, New York.

- [28] Entingh, DJ, Easwaran, E & McLarty, L 1994, 'Small Geothermal Electric Systems for Remote Powering', *Geothermal Resources Council Transactions*, vol. 18, no. 1, pp. 39-46.
- [29] Bejan, A 1988, *Advanced Engineering Thermodynamics*, Wiley, New York.
- [30] Sonntag, RE, Borgnakke, C & Van Wylen, GJ 2003, *Fundamentals of thermodynamics*, John Wiley, New York.
- [31] Zimparov, V 2001, 'Extended performance evaluation criteria for enhanced heat transfer surfaces: heat transfer through ducts with constant heat flux', *International Journal of heat and Mass Transfer*, vol. 44, no. 1, pp. 169-180.
- [32] Gnielinski, V 1983, 'Forced convection in ducts', in Spalding, DB & Taborek, J, *Heat Exchanger Design Handbook*, Hemisphere Publishing Corporation, Dusseldorf, pp. 2.5.1-1 to 2.5.1-10.
- [33] Kanoglu, M 2002, 'Exergy analysis of a dual-level binary geothermal power plant', *Geothermics*, vol. 31, no. 1, pp. 709-724.
- [34] Subbiah, S & Natarajan, R 1988, 'Thermodynamic analysis of binary-fluid rankine cycles for geothermal power plants', *Energy Conversion and Management*, vol. 28, no. 1, pp. 47-52.

## List of figures

Figure 1: (a) Binary cycle power plant with (b) hot-dry-rock geothermal reservoir

Figure 2: Variation of the ratio of pressure drops with the svelteness for different Reynolds numbers

Figure 3: Maximum first- and second-law efficiency as a function of the geothermal rejection temperature

Figure 4: Optimum mass flow rate of the geothermal fluid with variation in temperature gradient

Figure 5: Optimum mass flow rate of the geothermal fluid with variation in the geothermal outlet temperature

Figure 6: Downhole heat exchanger outer diameter with variation in temperature gradient

Figure 7: Downhole heat exchanger outer diameter with variation in the geothermal outlet temperature

Figure 8: Minimum entropy generation rate per unit length with variation in temperature gradient

Figure 9: Maximum first- law efficiency as a function of the geothermal rejection temperature

Figure 10: Maximum second- law efficiency as a function of the geothermal rejection temperature

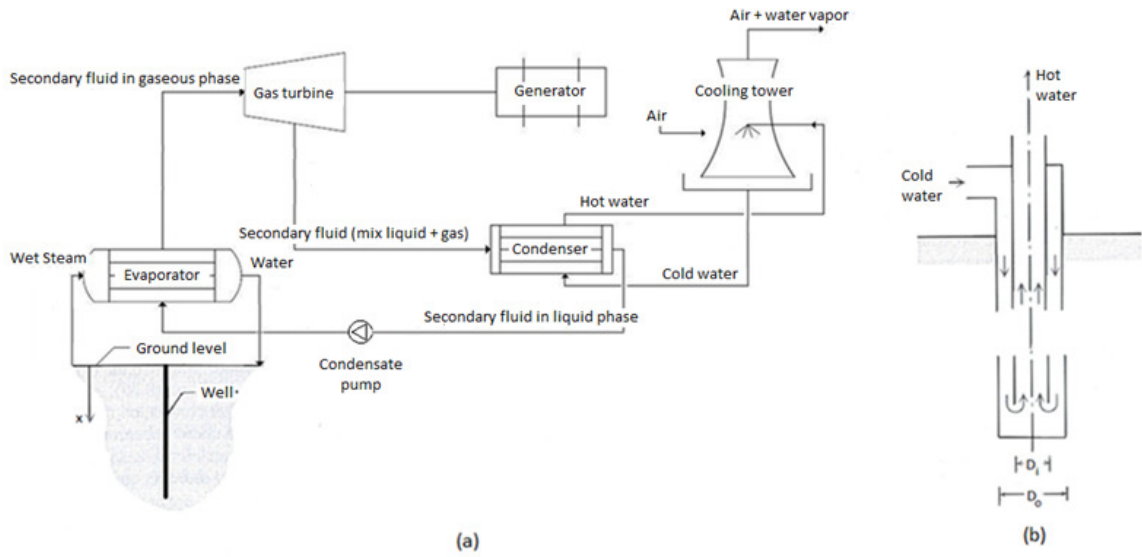


Figure 1

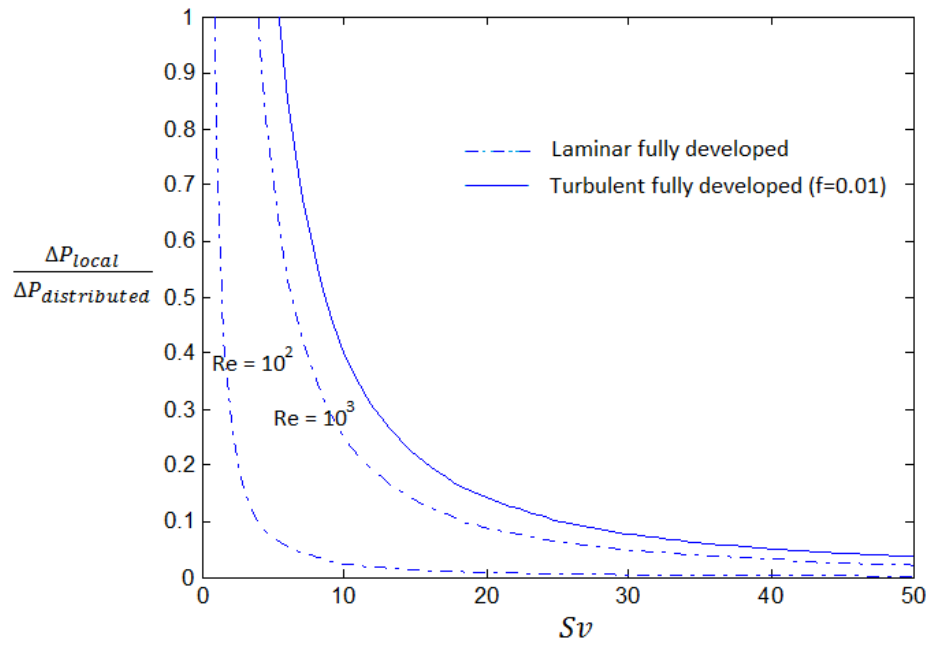


Figure 2

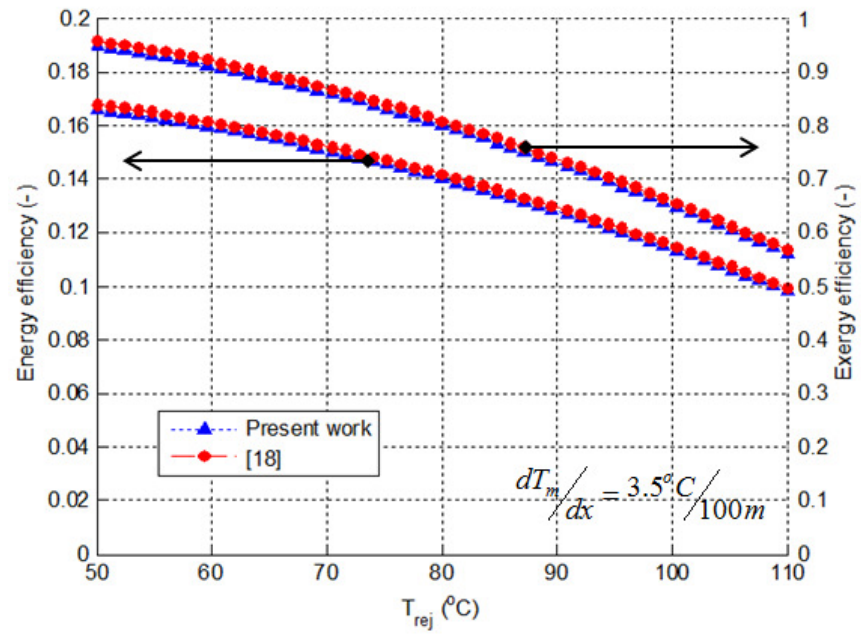


Figure 3

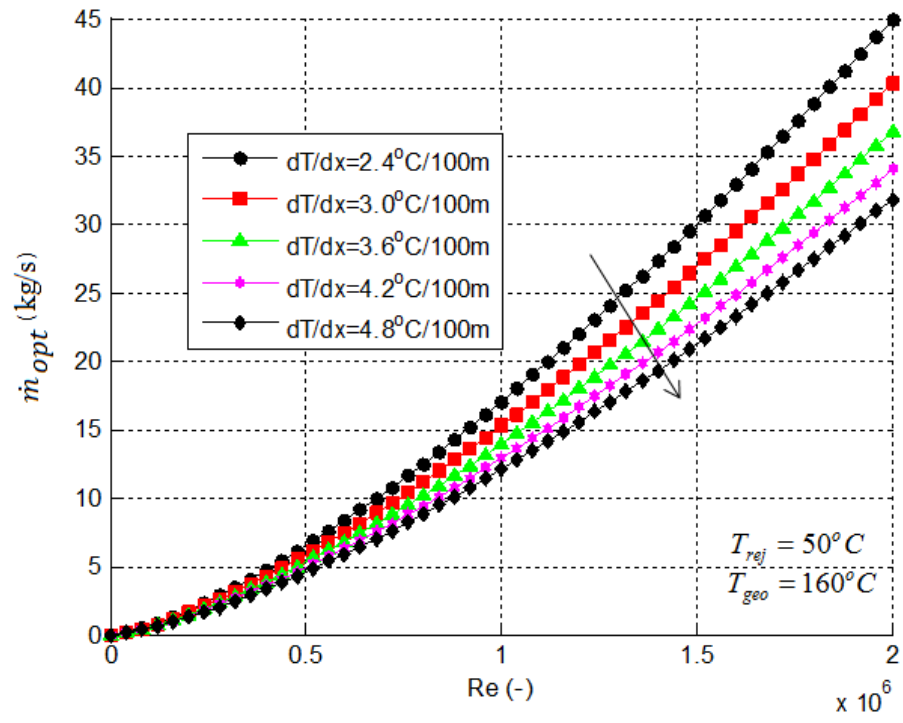


Figure 4

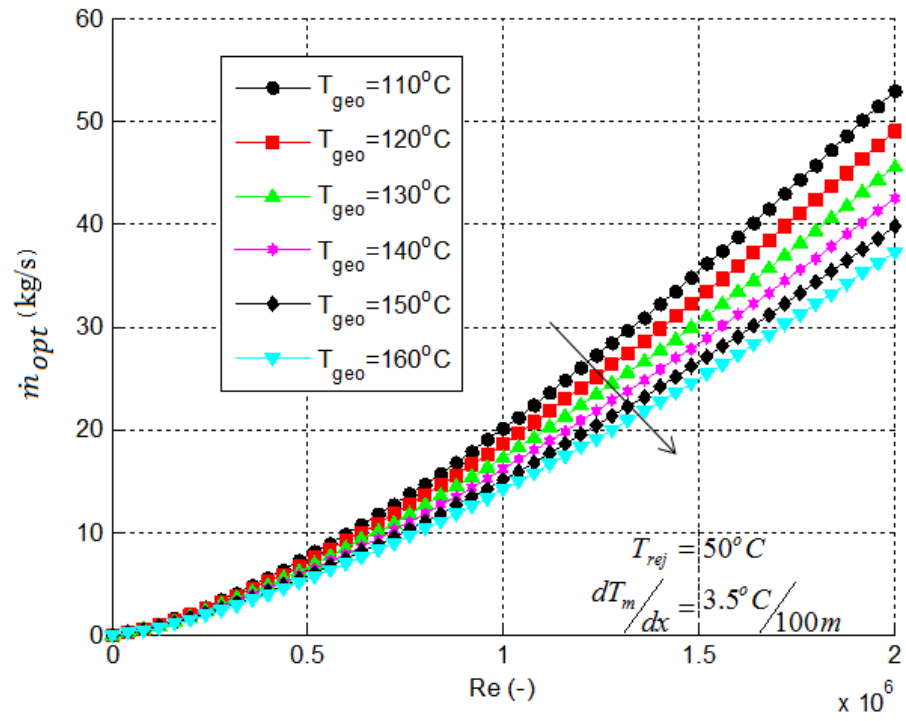


Figure 5

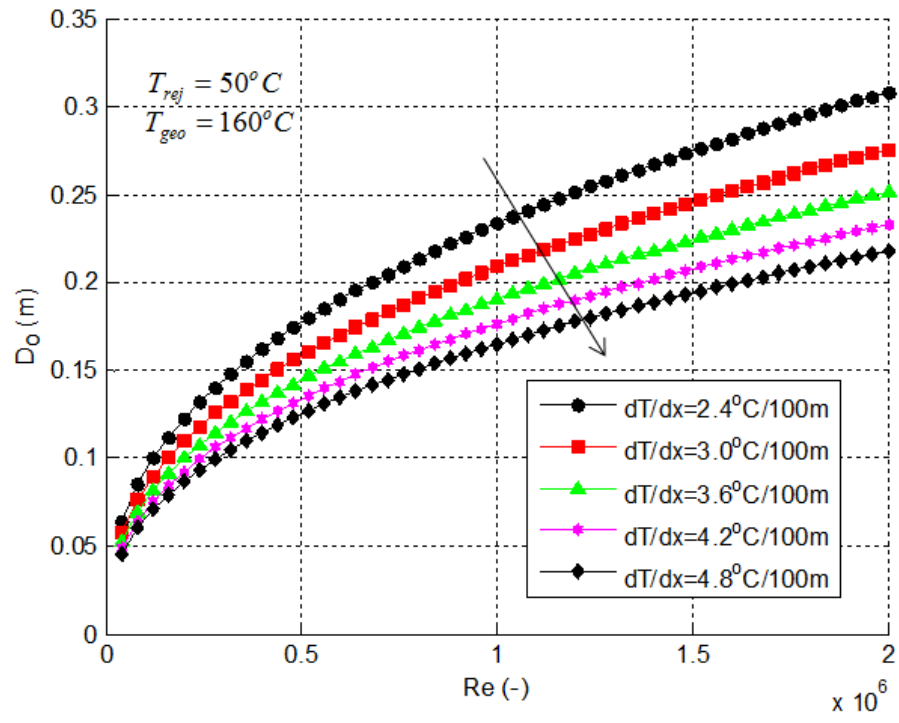


Figure 6

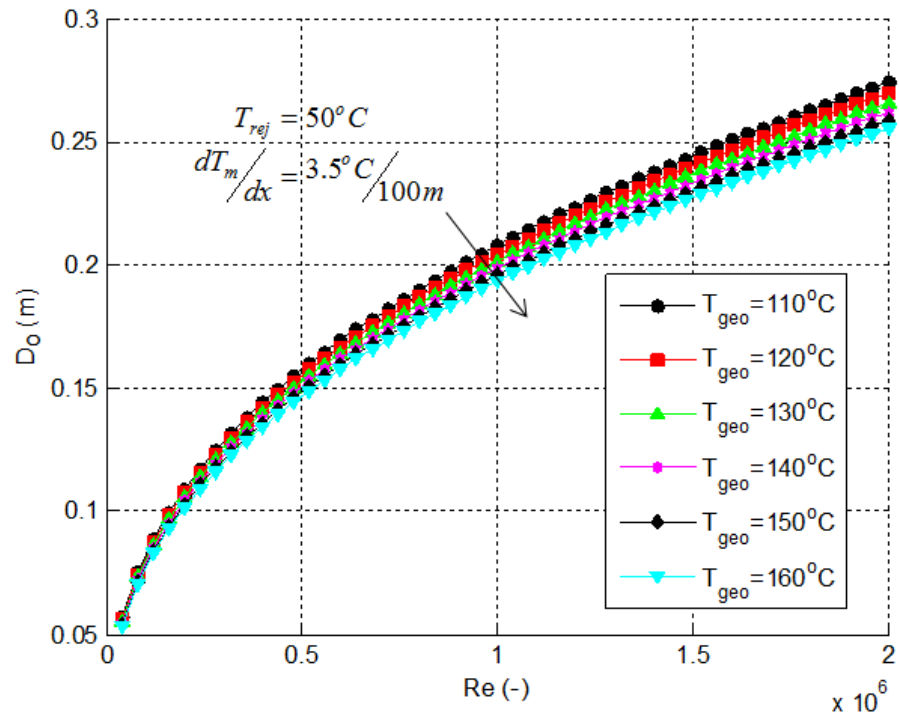


Figure 7

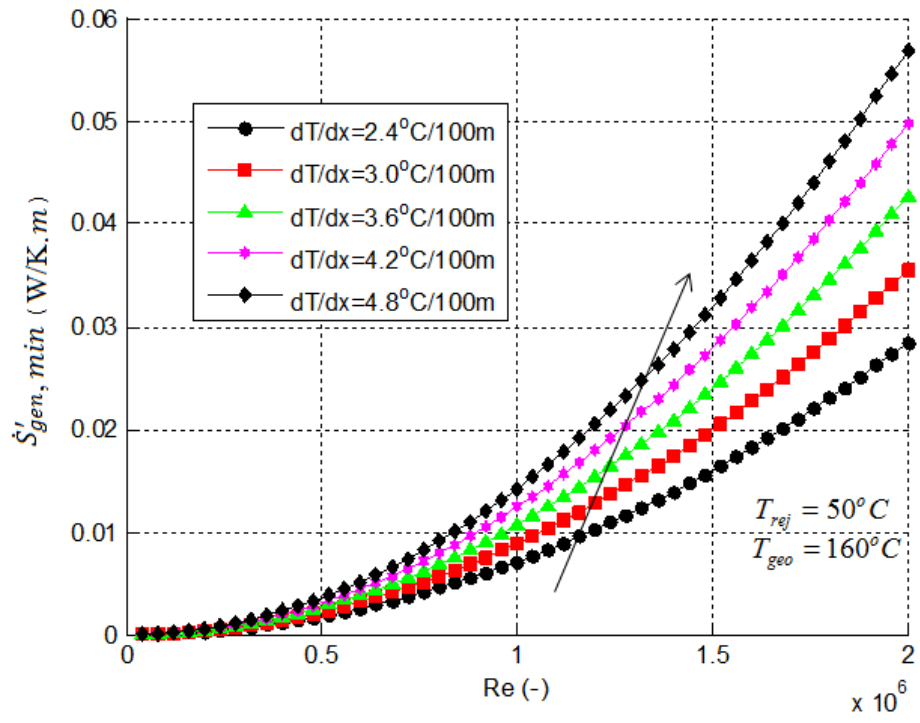


Figure 8

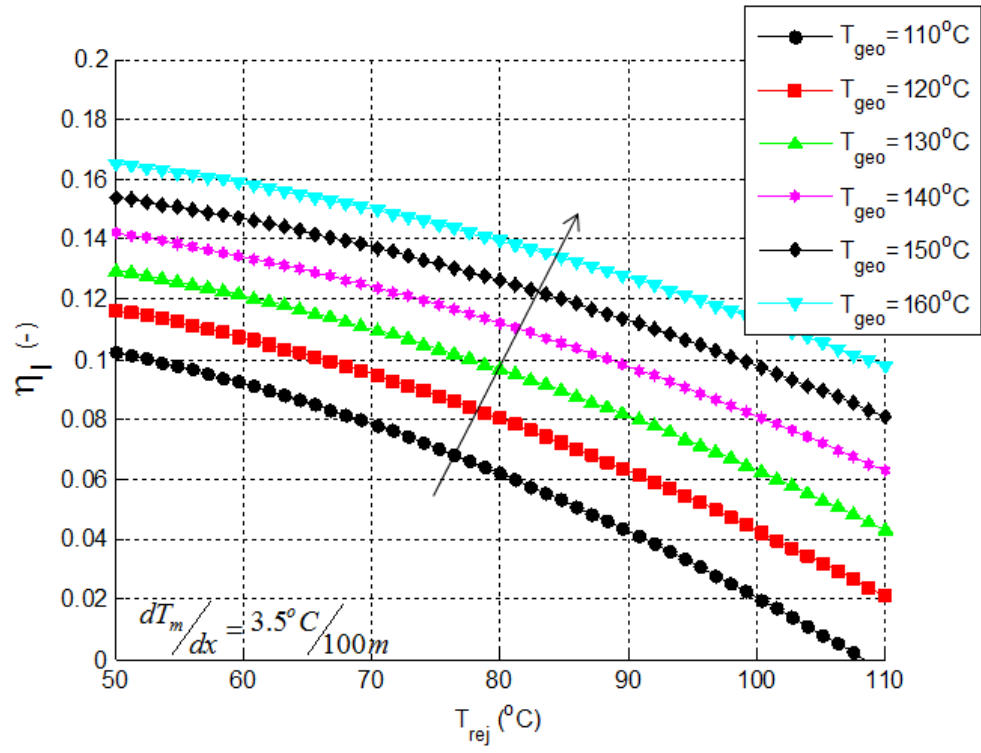


Figure 9

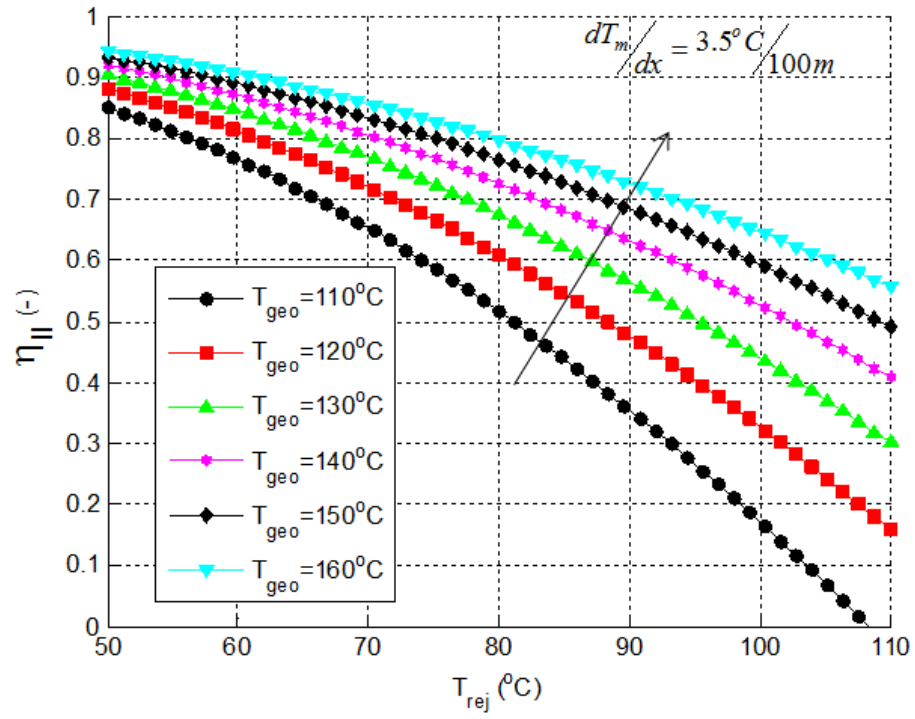


Figure 10